Radiative lifetimes of several metastable states of doubly and triply ionized Ar, Kr, and Xe

Anthony G. Calamai* and Charles E. Johnson
Physics Department, North Carolina State University, Raleigh, North Carolina 27695
(Received 13 January 1992)

The natural radiative lifetimes of the $ns^2np^4\,(^1S_0)$ metastable states of Ar^{2+}, Kr^{2+}, and Xe^{2+} with $n = 3$, 4, or 5, respectively, have been measured using an ion-trapping technique. In addition, we have measured the natural radiative lifetimes of the $4s^24p^3\,(^2P_{1/2})$ metastable state of Kr^{3+} and also of the $5s^25p^3\,(^2P_{1/2}$ and $^2P_{3/2})$ metastable states of Xe^{3+}. The decay rate of each state was determined by counting for equal time intervals the uv photons emitted as the metastable ion population decayed to a lower level of the ground-state configuration. A population of ions was produced inside a cylindrical electrostatic ion trap by electron bombardment of the appropriate parent gas maintained at pressures ranging from 4 to 80 $\times$ 10^{-8} Torr. The trap consisted of a 5.0-cm-diam, 7.5-cm-long cylinder with end caps plus a concentric 0.003-cm-diam central cylinder maintained at a negative potential of 150 V. Following electron impact of the parent gas, some of the photons emitted by the decaying metastable ion population were focused onto a narrow-bandwidth interference filter. Photons transmitted by the filter were detected by a photomultiplier tube as a function of time and generated a decay curve. As dictated by the composition of the photon decay curve, the pressure-dependent decay rate of each metastable state was obtained from a least-squares fit of either a single- or double-component exponential decay to the natural logarithm of its decay curve. The mean decay rate was extrapolated to zero pressure of the parent gas using a straight-line least-squares fit, and the inverse of the zero-pressure intercept yields the natural radiative lifetime of the relevant metastable state. Our measurements for the $^1S_0$ metastable states of Ar^{2+}, Kr^{2+}, and Xe^{2+} yield 133 $\pm$ 24, 14.8 $\pm$ 0.8, and 4.6 $\pm$ 0.3 msec for the natural radiative lifetime of the respective metastable state. Our result for the lifetime of the $^2P_{1/2}$ metastable state of Kr^{3+} is 47 $\pm$ 5 msec, while the lifetimes of the $^2P_{1/2}$ and $^2P_{3/2}$ metastable states of Xe^{3+} are 15.6 $\pm$ 0.9 and 5.3 $\pm$ 0.5 msec, respectively.

PACS number(s): 32.70.Fw

I. INTRODUCTION

Within an atomic electron configuration, the combined spin-orbit and electron-electron interactions produce a manifold of energy levels all with the same parity. Thus, excited levels of a ground-state configuration are rigorously forbidden by the parity selection rule to undergo spontaneous decay by an electric dipole ($E1$) transition. Such excited states, known as metastable states, give rise to weak spectral lines as they decay via magnetic dipole ($M1$) and electric quadrupole ($E2$) transitions. Metastable states of low-charge-state atomic ions have radiative transition probabilities typically four to eight orders of magnitude less than allowed $E1$ transitions. We have used an ion-trapping technique [1, 2] to measure the natural radiative lifetimes of the $ns^2np^4\,(^1S_0)$ metastable states of Ar^{2+}, Kr^{2+}, and Xe^{2+} with $n = 3$, 4, or 5, respectively. In addition, we have measured the radiative lifetimes of the $4s^24p^3\,(^2P_{1/2})$ metastable state of Kr^{3+} and also of the $5s^25p^3\,(^2P_{1/2}$ and $^2P_{3/2})$ metastable states of Xe^{3+}. Unfortunately, we were unable to measure the lifetime of the $4s^24p^3\,(^2P_{3/2})$ metastable state of Kr^{3+} since the appropriate transition for monitoring the decay of this state is not sufficiently isolated from a forbidden transition in Kr^{2+}.

The energy levels [3] of the $4s^24p^4$ ground-state configuration of Kr^{2+} are shown in Fig. 1. Except for an inversion of the $^3P_1$ and $^3P_0$ levels in Xe^{2+}, the energy levels [3, 4] of the ground-state configurations of Ar^{2+} and Xe^{2+} are similar to those of Kr^{2+}. Theoretical values [4–8] of the transition probabilities for the $^1S_0$ metastable state give natural radiative lifetimes of about 150, 17, and 5 msec for Ar^{2+}, Kr^{2+}, and Xe^{2+} respectively. For all three ions, the $(^1S_0 \rightarrow {}^3P_1)$ $M1$ transition, indicated by the solid line in Fig. 1, is the dominant decay branch of the $^1S_0$ metastable state and represents 60% of the total transition probability [5–7] in Ar^{2+} and greater than 90% in both [8] Kr^{2+} and Xe^{2+}. Photons emitted during the $(^1S_0 \rightarrow {}^3P_1)$ transition have wavelengths of approximately 311, 350, and 380 nm for Ar^{2+}, Kr^{2+}, and Xe^{2+} respectively. One previous measurement of the natural radiative lifetime exists for the $^1S_0$ metastable state of each ion. Prior [9] determined a lifetime of 109 $\pm$ 27 msec for the $^1S_0$ state of Ar^{2+}. Later, Walch and Knight [10] measured the lifetime of this state for both Kr^{2+} and Xe^{2+}, obtaining values of 13.1 $\pm$ 0.6 and 4.5 $\pm$ 0.3 msec respectively.

The energy levels [3, 11] of the $5s^25p^3$ ground-state configuration of Xe^{3+} are shown in Fig. 2. The more recent analysis [11] of the Xe^{3+} spectrum showed that the energy of the $5s^25p^3\,(^2P_{3/2})$ level was about 0.77 eV higher than the earlier tabulated value [3]; our results support

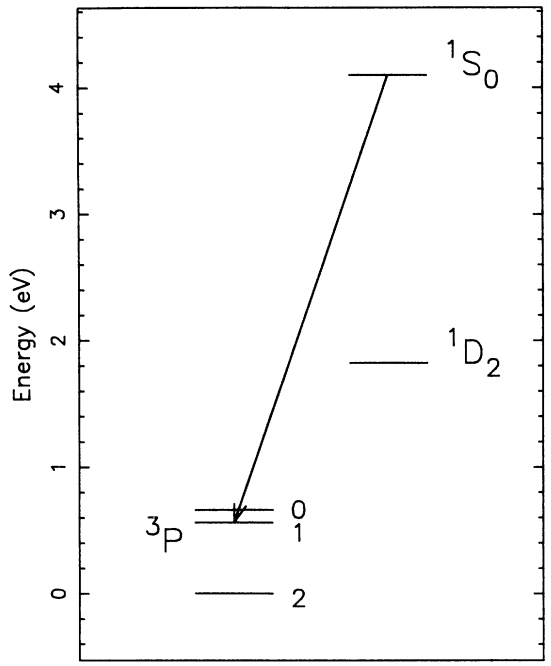

FIG. 1. Kr^{2+} energy-level diagram showing the five energy levels of the $4s^24p^4$ ground-state configuration. The solid line indicates the forbidden transition monitored for the measurement of the natural radiative lifetimes of the $^1S_0$ metastable state of Ar^{2+}, Kr^{2+}, and Xe^{2+}.

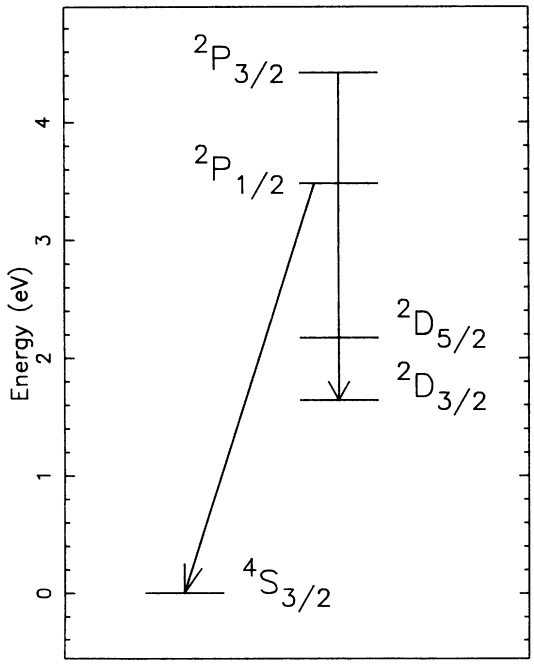

FIG. 2. Xe^{3+} energy-level diagram showing the five energy levels of the $5s^25p^3$ ground-state configuration. The solid lines indicate the forbidden transitions monitored for the measurement of the natural radiative lifetimes of the metastable states.

this reassignment of the Xe^{3+} ($^2P_{3/2}$) level. The energy levels [3, 12] of the $4s^24p^3$ ground-state configuration of Kr^{3+} are similar to those of Xe^{3+}. The calculated transition probabilities [13, 14] for the energy levels of the $4s^24p^3$ configuration of Kr^{3+} predict natural radiative lifetimes of approximately 55 and 23 msec, respectively, for the $4s^24p^3$ ($^2P_{1/2}$ and $^2P_{3/2}$) metastable states, while those [14] for the energy levels of the $5s^25p^3$ configuration of Xe^{3+} predict natural radiative lifetimes of approximately 16 and 7 msec, respectively, for the $5s^25p^3$ ($^2P_{1/2}$ and $^2P_{3/2}$) metastable states. For both Kr^{3+} and Xe^{3+}, the ($^2P_{1/2} \rightarrow {}^4S_{3/2}$) and ($^2P_{3/2} \rightarrow {}^2D_{3/2}$) $M1, E2$ transitions, indicated by the solid lines in Fig. 2, are expected to be the dominant decay branches [13, 14] of the $^2P_{1/2}$ and $^2P_{3/2}$ metastable states. In Xe^{3+}, for example, the ($^2P_{1/2} \rightarrow {}^4S_{3/2}$) transition at 357 nm represents 83% of the $^2P_{1/2}$ state's total transition probability, while the ($^2P_{3/2} \rightarrow {}^2D_{3/2}$) transition at 447 nm is responsible for 53% of the total transition probability for the $^2P_{3/2}$ state.

II. EXPERIMENTAL METHOD

Since our experimental apparatus has been discussed previously [2], only a brief review of the ion trap and our experimental method is given. An ion population, produced by electron impact of the appropriate parent atom gas, was confined to a volume of approximately 25 cm^3 by the electric fields of a cylindrical electrostatic ion trap [1, 15, 16]. The electrostatic ion trap and a 0.5-in-diam tungsten dispenser cathode were located in a vacuum chamber where the residual background pressure, as measured by an uncalibrated Baynard-Alpert ionization gauge, was approximately 10^{-9} Torr. Parent atoms were admitted to the vacuum chamber through an adjustable leak valve and set to pressures that ranged from 4 to 80 $\times$ 10^{-8} Torr. Two circular ports, located on the 5-cm-diam outer electrode of the trap, were covered with tungsten wire cloth to allow the photons emitted by the decaying metastable ions to be observed. The trap's end caps were also constructed using tungsten wire cloth so that electrons from the hot cathode could pass through the trap. These electrons, accelerated to about 200 eV just before entering the trap, traveled parallel to the trap's axis and produced various ionization states of the parent atoms inside the trap by electron impact. Assuming an estimated photon counting efficiency of 0.1%, the observed signals indicate that for each fill pulse approximately 10^4 Ar^{2+}, Kr^{2+}, or Xe^{2+} ions were created in the $^1S_0$ metastable state and that about 10^3 ions of the desired metastable state of Kr^{3+} or Xe^{3+} were created.

After the trap was filled, some of the photons emitted by the decaying metastable ion population passed through a port in the outer cylindrical electrode and were focused onto a narrow-bandwidth interference filter positioned in front of a photomultiplier tube. The interference filter preferentially selected photons emitted by the state of interest and also rejected unwanted background radiation emitted by the hot dispenser cathode. Characteristics of the interference filters used in these metastable lifetime measurements are shown, along

TABLE I. Wavelengths of the transitions monitored, and also characteristics of the interference filters used, for the metastable-state lifetime measurements. Transition wavelengths, positions of maximum filter transmittance (peak λ), and full width at half maximum (FWHM) values of the filters are given in nanometers. The Peak $\%T$ column lists the percent transmittance of each filter at its peak λ.

Ion	Transition	Wavelength	Peak λ	FWHM	Peak $\%T$
Ar^{2+}	$^1S_0 \rightarrow {}^3P_1$	311	312 ± 1	10 ± 1	27 ± 2
Kr^{2+}	$^1S_0 \rightarrow {}^3P_1$	350	350 ± 1	10 ± 1	52 ± 2
Xe^{2+}	$^1S_0 \rightarrow {}^3P_1$	380	380 ± 1	8 ± 1	20 ± 2
Kr^{3+}	$^2P_{1/2} \rightarrow {}^4S_{3/2}$	322	323 ± 1	11 ± 1	33 ± 2
Xe^{3+}	$^2P_{1/2} \rightarrow {}^4S_{3/2}$	357	360 ± 1	10 ± 1	27 ± 2
Xe^{3+}	$^2P_{3/2} \rightarrow {}^2D_{3/2}$	447	449 ± 1	10 ± 1	22 ± 2

with the transitions monitored, in Table I. The transmittance curve of each filter was quite steep near the peak transmittance wavelength, and the transmittance was less than ~0.25%, 12 nm to either side of the peak wavelength.

Counts associated with the decay of a particular metastable state were collected through a cycle consisting of five events: a fill pulse, two photon counting periods, and two trap dumps. The trap was emptied, or dumped, of ions by applying a positive voltage pulse for 1 msec to the central electrode of the trap. The photon counting periods consisted of either 50 or optionally 100 channels of equal temporal width. Thus each photon counting period defined a scan whose time duration equaled the product of channel width and the number of channels. Table II summarizes the timing parameters that were used.

At the beginning of each channel, an on-line computer zeroed and gated on a 32-bit counter to register the number of photons detected as the metastable ion population inside the trap radiatively decayed. Counts accumulated during a channel's dwell time were read by the computer and stored in a separate memory location for each channel. Signal averaging with background subtraction was accomplished by using two photon counting periods per cycle and repeating the cycle many times. The first photon counting period, which was preceded by a fill pulse, contained a record of both signal and background counts, while the second photon counting period, which was preceded by a trap dump, corresponded to only background counts. The counts collected in the second counting period were subtracted from the number detected during the first period on a channel-by-channel basis and the result was added to that of previous cycles. Therefore, the signal level of each channel was accumulated and the background was minimized. At the conclusion of a data collection run, the signal emitted by the trapped ions had been recorded versus time and predominantly consisted of counts arising from the stored metastable ion population. For these measurements, integration times for each data run ranged from a low of ~ 6 h for the Xe^{2+} ($^1S_0$) metastable state to a high of ~ 21 h for the Kr^{3+} ($^2P_{1/2}$) metastable state.

Each radiative lifetime measurement commenced with a few preliminary runs for diagnostic purposes where parameters affecting signal quality were varied. Results of the diagnostic runs were analyzed in order to determine an approximate value for the lifetime to be measured, ascertain whether or not more than one decay component existed in the decay curve, and also to choose run parameters that would simultaneously maximize signal quality while minimizing total run time. After the diagnostic runs were analyzed, integration times, channel widths, and the number of channels were chosen so that the total photon counting interval spanned approximately four mean lifetimes or until the signal level in the last few channels was about the same size as the background noise. In a series of separate experiments, the total ion storage time was determined at each pressure of each parent gas used in the lifetime measurements and was found, at a minimum, to be at least twice the measured radiative lifetime of the revelant metastable state.

TABLE II. Timing parameters (in milliseconds) used for the natural radiative lifetime measurements. The quotient (scan duration/channel width) gives the number of channels per scan for each measurement.

Ion	State	Fill period	Channel width	Scan duration
Ar^{2+}	$^1S_0$	100.0	6.0	300.0
Kr^{2+}	$^1S_0$	40.0	1.0	50.0
Xe^{2+}	$^1S_0$	20.0	0.4	20.0
Kr^{3+}	$^2P_{1/2}$	30.0	0.6	60.0
Xe^{3+}	$^2P_{1/2}$	20.0	0.7	35.0
Xe^{3+}	$^2P_{3/2}$	20.0	0.5	50.0

III. DATA ANALYSIS

For a metastable-state population decaying according to the exponential $N_0e^{-\gamma t}$, the natural logarithm of the decay counts versus time is a straight line whose slope is the decay rate γ. Neglecting the first few channels of the decay where the ion cloud stabilizes and allowed cascades occur, Fig. 3 shows the expected straight-line behavior for the logarithmic plot of decay counts associated with the decay of stored Xe^{2+} ($^1S_0$) ions. However, as shown in Fig. 4, the logarithm of the decay counts collected for the Kr^{3+} ($^2P_{1/2}$) lifetime measurement deviates significantly from a single-component exponential decay.

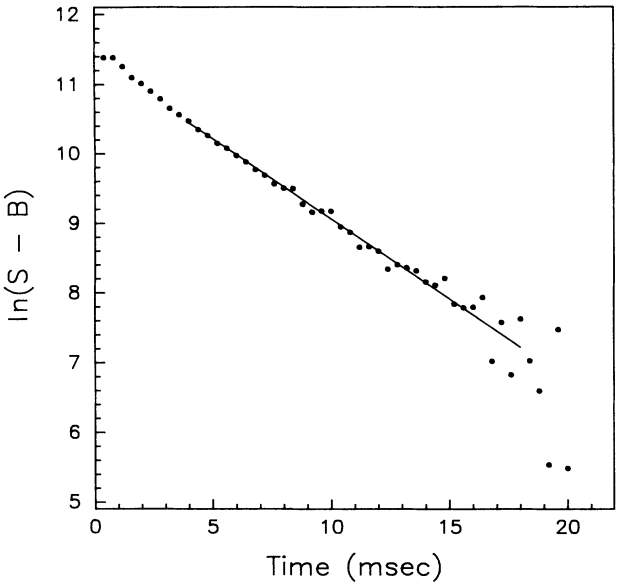

FIG. 3. 50-channel decay curve showing the natural logarithm of signal counts S minus background B vs time as the $5s^25p^4$ ($^1S_0$) metastable-state population of Xe^{2+} decays. An interference filter centered at 380 nm was used to monitor the 380-nm photons emitted as a result of the ($^1S_0 \rightarrow {}^3P_1$) $M1, E2$ transition. The slope of a straight-line (solid line) least-squares fit to the data gives the decay rate of the Xe^{2+}($^1S_0$) metastable state.

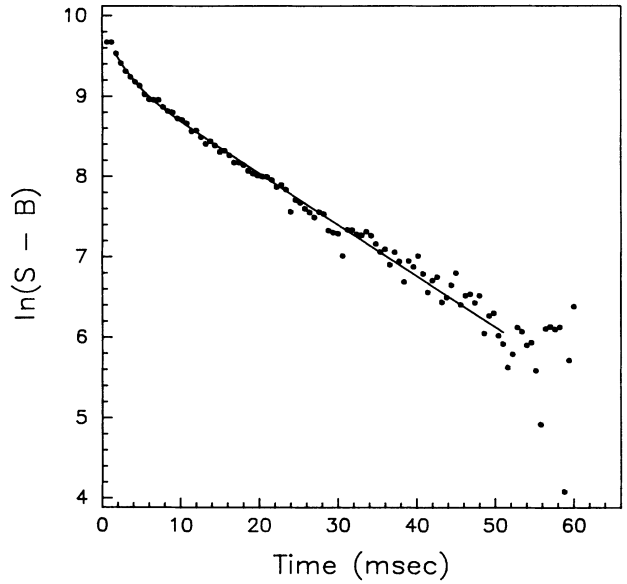

FIG. 4. 100-channel decay curve showing the natural logarithm of signal counts S minus background B vs time as the $4s^24p^3$ ($^2P_{1/2}$) metastable-state population of Kr^{3+} decays. An interference filter centered at 323 nm was used to monitor the 322-nm photons emitted as a result of the ($^2P_{1/2} \rightarrow {}^4P_{3/2}$) $M1, E2$ transition. The solid line results from a nonlinear least-squares fit of $\ln(S - B)$ to two exponentially-decaying populations. The slower decaying component corresponds to the decay of the Kr^{3+}($^2P_{1/2}$) metastable state while the faster decaying component reflects both cascades from higher levels and ion cloud stablization after the end of the electron bombardment of the neutral Kr parent gas.

When the decay curve contains only a single component, the decay rate γ is obtained from the slope of a straight-line fit to the appropriate region of the natural logarithm of the decay counts using a weighted least-squares-fitting procedure [17]. But, when the decay curve consists of two components, a weighted four-parameter least-squares fit to the logarithm of two exponentially decaying populations is used instead. Then the decay counts versus time are modeled by

$$N(t) = N_1 e^{-\gamma_1 t} + N_2 e^{-\gamma_2 t}, \tag{1}$$

where N_1, N_2 are the two initial populations and γ_1, γ_2 the two decay rates. Initially, all decay curves were fit with both the single- and double-component decay models. However, we found that only the decay curves for the Kr^{3+} ($^2P_{1/2}$) and Xe^{3+} ($^2P_{3/2}$) metastable states required fitting to the double-component model. In all cases, the first few channels of each decay curve were excluded from the least-squares-fitting procedure in order to minimize the effects of ion cloud stablization and cascades from higher levels, while the last few channels were used to determine the small residual background that was not removed by the real-time background subtraction technique discussed in Sec. II.

The total decay rate γ consists of two parts: the radiative decay rate γ_0 plus a pressure-dependent decay rate γ_p that represents all losses of the metastable ions as a consequence of collisions with the neutral parent atoms present in the trapping volume. To first order in parent atom pressure P, the decay rate is

$$\gamma = \gamma_0 + \gamma_p = \gamma_0 + k\, n_p, \tag{2}$$

where k is the collision rate coefficient and n_p is the number density of the appropriate parent atoms per unit volume at a particular pressure P. For each metastable state whose lifetime was being measured, we accumulated numerous decay curves at various parent pressures. Then the zero-pressure intercept of a straight line least-squares fit to a plot of the decay rate versus pressure is the radiative decay rate γ_0, and the natural radiative lifetime τ_0 of the metastable state producing the decay curve is $\tau_0 = 1/\gamma_0$. Moreover, the slope of the straight line gives the collision rate coefficient k.

IV. RESULTS

A. $^1S_0$ metastable state of Ar^{2+}, Kr^{2+}, and Xe^{2+}

Except for the first few milliseconds of the decay where the ion cloud stablizes and allowed cascades occur, decay curves taken for the lifetime measurements of the $^1S_0$ metastable states of Ar^{2+}, Kr^{2+}, and Xe^{2+} exhibited only a single exponentially-decaying component. As an example, Fig. 3 shows a logarithmic plot of a decay curve accumulated for the Xe^{2+} ($^1S_0$) metastable state.

Our result for the lifetime of this state is based on 38 decay curves that were collected at Xe parent pressures ranging from 10 to 50 × 10^{-8} Torr. The integration time for each Xe^{2+} decay curve was approximately 6 h. As shown by the solid line in Fig. 3, the decay rate was obtained from a least-squares fit to the time interval from 4 to 18 msec after the end of the electron-bombardment period. After extrapolation of the decay rates to zero Xe pressure as shown in Fig. 5, we find that the natural radiative lifetime of the $5s^25p^4\,(^1S_0)$ metastable state of Xe^{2+} is 4.6 ± 0.3 msec.

Our final measured value for the lifetime of the $4s^24p^4\,(^1S_0)$ metastable state of Kr^{2+} is based on a total of 119, 9-h runs taken at the same Kr parent pressures as those used for the $Xe^{2+}\,(^1S_0)$ lifetime measurement. As a check for possible systematic effects associated with ion cloud stabilizaton, half of the decay curves were collected with a 50-G magnetic field applied coaxially with the ion trap. However, using the time interval from 5 to 35 msec after the end of the fill pulse as the least-squares-fit region, there was no significant difference in the decay rates with or without the magnetic field. Therefore, all the decay rates were combined and then extrapolated to zero Kr pressure, as shown in Fig. 6. The resulting value for the natural radiative lifetime of the $Kr^{2+}\,(^1S_0)$ metastable state is 14.8 ± 0.8 msec.

A total of 73, 9-h decay curves for the $3s^23p^4\,(^1S_0)$ metastable state of Ar^{2+} were accumulated at Ar pressures ranging from 6 to 16 × 10^{-8} Torr. A single-component exponential was least-squares fit to each decay curve for the time interval from 30 to 210 msec, with the last few channels once again being used to determine the residual background counts. Although we have not included a plot of the decay rates versus pressure, extrapolation of the mean decay rates to zero Ar pressure gives our result of 133 ± 24 msec for the natural radiative lifetime of the $Ar^{2+}\,(^1S_0)$ metastable state.

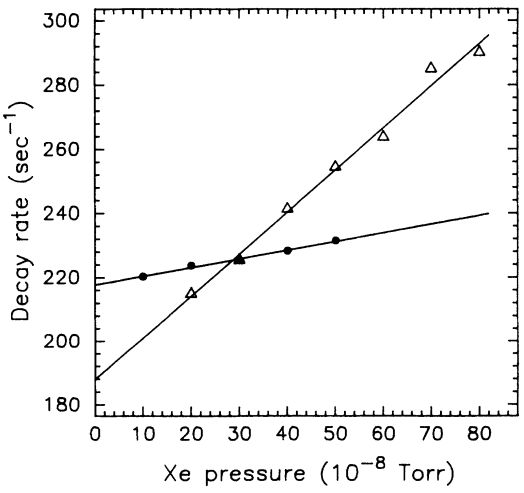

FIG. 5. Decay rates vs parent Xe pressure for both the $5s^25p^4\,(^1S_0)$ metastable state of Xe^{2+} and the $5s^25p^3\,(^2P_{3/2})$ metastable state of Xe^{3+}; •, $^1S_0$ state; △, $^2P_{3/2}$ state. The natural radiative lifetimes are obtained from the zero-pressure intercepts of the relevant straight-line fit, whereas collision rate coefficients are deduced from the slopes.

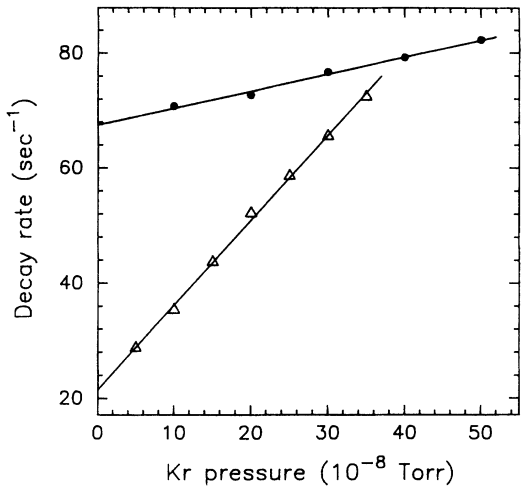

FIG. 6. Decay rates vs parent Kr pressure for both the $4s^24p^4\,(^1S_0)$ metastable state of Kr^{2+} and the $4s^24p^3\,(^2P_{1/2})$ metastable state of Kr^{3+}; •, $^1S_0$ state; △, $^2P_{1/2}$ state. The natural radiative lifetimes are obtained from the zero-pressure intercepts of the relevant straight-line fit, whereas collision rate coefficients are deduced from the slopes.

Our results for the radiative lifetimes of the $^1S_0$ metastable state of Ar^{2+}, Kr^{2+}, and Xe^{2+} are compared in Table III with previous experimental and theoretical values. The agreement is quite satisfactory in the case of Ar^{2+} and Xe^{2+}; however, for Kr^{2+} there is a mild discrepancy between both experimental values and also the theoretical values, although the errors of the theoretical calculations are unknown.

B. Metastable states of Kr^{3+} and Xe^{3+}

A total of 45 decay curves for the $4s^24p^3(^2P_{1/2})$ metastable state of Kr^{3+} were accumulated at Kr parent pressures ranging from 5 to 35 × 10^{-8} Torr. As shown in Fig. 4 where the natural logarithm of the decay counts is plotted versus time, at least two decay rates are associated with the decay curve; the solid curve shown in Fig. 4 represents a nonlinear, two-component, least-squares fit to the natural logarithm of the decay counts for the time interval from 2 to 54 msec after the end of the fill pulse. However, in contrast to the other metastable states of interest as well as to earlier measurements [2,18] of metastable state lifetimes, the pressure dependence of the faster component's decay rate is not characteristic of a radiative decay process since the decay time, as determined by the two-component fit, increases with Kr parent pressure. But, as shown in Fig. 6, a plot of the slower component's decay rates versus Kr parent pressure yields the expected straight-line behavior and as discussed later,

TABLE III. Comparison of the values for the natural radiative lifetimes (in milliseconds) of the $^1S_0$ metastable state of Ar^{2+}, Kr^{2+}, and Xe^{2+}.

Authors	Ar^{2+}	Kr^{2+}	Xe^{2+}	
Garstang[a]		17.2	4.4	theory
Mendoza and Zeippen[b]	153			theory
Czyzak and Krueger[c]	140			theory
Hansen and Persson[d]			4.9	theory
Biémont and Hansen[e]	149	17.3		theory
Prior[f]	109 ± 27			experiment
Walch and Knight[g]		13.1 ± 0.6	4.5 ± 0.3	experiment
This work	133 ± 24	14.8 ± 0.8	4.6 ± 0.3	experiment

[a]Reference [8].
[b]Reference [5].
[c]Reference [6].
[d]Reference [4].
[e]Reference [7].
[f]Reference [9].
[g]Reference [10].

a collision rate coefficient significantly larger than for the Kr^{2+} ($^1S_0$) metastable state. This larger collision rate coefficient indicates that the slower component is a radiative process originating from a population of Kr ions in an ionization state greater than Kr^{2+}. Therefore, we consider the slower component to represent the decay of the Kr^{3+} ($^2P_{1/2}$) metastable state; we suspect that the faster component arises from collisions and/or cascades involving parent Kr atoms and the stored ions (Kr^{1+}, Kr^{2+}, Kr^{3+}, and perhaps Kr^{4+}). The longest measured decay time of the faster component was less than 3 msec, and a single-component fit (straight line) to the natural logarithm of the decay counts for the time interval from 15 to 54 msec gives, to within the statistical error of each theoretical fit, a decay rate consistent with the slower component of the double-component fit. Extrapolating the decay rates versus Kr pressure shown in Fig. 6 to zero parent pressure, we obtain 47 ± 5 msec for the natural radiative lifetime of the $4s^24p^3$ ($^2P_{1/2}$) metastable state of Kr^{3+}.

In order to determine the natural lifetime of the $5s^25p^3$ ($^2P_{1/2}$) metastable state of Xe^{3+}, 60 decay curves, each requiring ~ 8 h, were collected at Xe pressures ranging from 4 to 50 × 10^{-8} Torr. As listed in Table I, the 357-nm radiation emitted by the decaying Xe^{3+} ($^2P_{1/2}$) metastable ion population was monitored using an interference filter centered at 360 nm. Although the transmittance of this filter was quite small beyond 375 nm, the possibility of 380-nm photons, emitted by the Xe^{2+} ($^1S_0$) metastable ion population, leaking through the 360-nm interference filter was of specific concern. As a test of this possibility, several additional decay curves were taken with all experimental parameters identical, except that the 350-nm interference filter described in Table I was used instead of the 360-nm filter. At a particular Xe pressure, the measured decay rates for decay curves collected with the 350-nm filter were the same, to within the statistical errors of the theoretical fits, as those collected with the 360-nm filter. The data clearly showed that only a single component was present in the decay, as confirmed by fitting the decay curves using both single- and double-component decay models. Correspondingly, decay rates were obtained from a straight-line least-squares fit to the natural logarithm of the decay counts for the time interval from 7 to 32 msec after the end of the fill pulse. The decay rates at each Xe pressure were averaged, and the mean decay rates were extrapolated to zero Xe pressure, yielding 15.6 ± 0.9 msec as the value for the lifetime of the Xe^{3+} ($^2P_{1/2}$) metastable state.

By monitoring the predominantly ($^2P_{3/2} \rightarrow {}^2D_{3/2}$) M1 transition at 447 nm, 58 decay curves, each requiring about 18 h, were collected for the $5s^25p^3$ ($^2P_{3/2}$) metastable state of Xe^{3+} at Xe pressures ranging from 20 to 80 × 10^{-8} Torr. Once again, at least two components were present in the decay curve. Since at each Xe pressure the extremely noisy slower component has about the same decay time as the ion storage time, we conclude that this component arises from photons generated as a consequence of collisional excitation of the parent Xe atoms by the stored ions, which are mostly ground-state Xe^+. Thus the faster component corresponds to the decay of the Xe^{3+} ($^2P_{3/2}$) metastable state. The logarithmic decay curves were fit by the two-component least-squares procedure on an interval from 3 to 43 msec after the end of the electron-bombardment period. The resulting mean decay rates of the faster component are plotted versus Xe pressure in Fig. 5; then the natural lifetime of the metastable state was obtained from the intercept at zero Xe pressure of a straight-line least-squares fit to the decay rates versus pressure. Our result for the natural radiative lifetime of the $5s^25p^3$ ($^2P_{3/2}$) metastable state of Xe^{3+} is 5.3 ± 0.5 msec.

Our experimental values for the natural radiative lifetimes of the $4s^24p^3$ ($^2P_{1/2}$) metastable state of Kr^{3+} and the $5s^25p^3$ ($^2P_{1/2}$ and $^2P_{3/2}$) metastable states of Xe^{3+} are compared in Table IV with the theoretical values. Although the measured lifetimes for a couple of the states are somewhat shorter than the predicted lifetimes, the agreement for all the metastable states is satisfactory.

C. Errors

One of the major concerns when making a direct measurement of the lifetime of a metastable state is that in addition to the transition of interest another tran-

TABLE IV. Comparison of the values for the natural radiative lifetimes (in milliseconds) of the $^2P_{1/2}$ and $^2P_{3/2}$ metastable states of Kr^{+3} and Xe^{+3}.

Authors	Ion	$^2P_{1/2}$	$^2P_{3/2}$	
Biémont and Hansen[a]	Kr^{+3}	55.2	23.3	theory
Reader[b]	Kr^{+3}	55.3	23.3	theory
	Xe^{+3}	15.8	6.6	
This work	Kr^{+3}	47 ± 5		experiment
	Xe^{+3}	15.6 ± 0.9	5.3 ± 0.5	

[a]Reference [13].
[b]Reference [14].

sition also will have a wavelength within the bandpass of the interference filter being used. In fact, this situation prevented the measurement of the lifetime of the $4s^24p^3\,(^2P_{3/2})$ metastable state of Kr^{3+}. However, for the other metastable states of interest, a second component having a small signal and/or similar decay rate might not be noticed and consequently could result in a substantial systematic error. A careful examination of the available data for the energy levels did not reveal any other metastable states of Ar, Kr, or Xe ions that might be produced in sufficient numbers so as to result in a systematic error in our measured radiative lifetimes. In order to check this conclusion experimentally for each parent gas, a set of narrow-bandwidth interference filters whose center wavelengths ranged from 200 to 450 nm was used to take a sequence of very long integration time runs over this entire spectral region. Except for spectral locations where known metastable transitions had some transmittance through the particular filter being used, the resulting scans gave only a constant flat background noise. As an additional check for undesired decay radiation, the same 200–450 nm wavelength range was investigated again, but without any parent gas present in the vacuum chamber. No decay signals were observed with any filter, just a flat background response. Other experimental parameters—such as trapping potential, electron-bombardment energy, trap fill time, and trap dump time—were varied also to explore for possible systematic errors. The measured decay rates were always the same to within the statistical errors of the theoretical fits.

The major source of error for our experimental lifetime values is an uncertainty associated with knowledge of the parent gas pressure and consequently the extrapolation of the measured decay rates to zero parent pressure. There is also some uncertainty associated with the particular choice of time interval for the theoretical fit and of the small amount of residual background that is subtracted. Combining these uncertainties, all considerably larger than the statistical errors, our estimated errors are presented in Tables III and IV along with the measured lifetime values.

D. Collision rate coefficients

The collision rate coefficients of the six metastable states of interest were determined from the slopes of the straight-line least-squares fit to the decay rates versus parent atom pressure; four examples are shown in Figs. 5 and 6. Actually, the pressure-dependent part γ_p of the total decay rate γ includes all pressure-dependent losses of ions from the metastable state and has at least two contributions. The first is the collisional quenching of the metastable state; the second is the loss of the metastable-state ion from the trap when a kinetic collision sufficiently perturbs its trajectory about the cylindrical center electrode of the trap. A separate measurement of the ion storage time [1] for loss of ions from the trap indicates that collisional quenching is the major contribution to γ_p. However, the ion storage time measurements are essentially for ground-state Ar^+, Kr^+, or Xe^+ since they are the dominant trapped ions. Nevertheless, the measured collision rate coefficients are listed in Table V and do show the expected increase in size as the ionization state of the parent atom increases.

Previous measurements [9, 10] of the collision rate coefficients for the $^1S_0$ metastable state of these doubly charged ions obtained values of 6×10^{-10} cm^3/sec for Ar^{2+}, 5×10^{-10} cm^3/sec for Kr^{2+}, and 3×10^{-10} cm^3/sec for Xe^{2+}. Our collision rate coefficients are larger than the previously determined values by a factor of 3 to 7. However, the earlier values as well as ours were deduced from pressure measurements obtained using uncalibrated ionization gauges, and this may introduce a substantial absolute error. Moreover, the velocity distributions of the stored ions in the ion traps used in the previous measurements may be different from that in our electrostatic

TABLE V. Measured collision rate coefficients k for the metastable states investigated. The uncalibrated ionization gauge used to measure the parent atom pressures may introduce an uncertainty of a factor of 2 or more for the absolute value of the rate coefficients, although the relative error is estimated to be about 25%.

Ion	Configuration	State	k (10^{-9} cm^3/sec)
Ar^{2+}	$3s^23p^4$	$^1S_0$	2.1
Kr^{2+}	$4s^24p^4$	$^1S_0$	1.6
Xe^{2+}	$5s^25p^4$	$^1S_0$	2.1
Kr^{3+}	$4s^24p^3$	$^2P_{1/2}$	8.0
Xe^{3+}	$5s^25p^3$	$^2P_{1/2}$	14.0
	$5s^25p^3$	$^2P_{3/2}$	9.9

trap. Given the uncertainties associated with the uncalibrated ionization gauges and the differing ion velocity distributions, our measured collision rates listed in Table V are consistent with the previously reported values.

V. SUMMARY

A list of the experimental and theoretical values for the natural radiative lifetimes of the $^1S_0$ metastable state of Ar^{2+}, Kr^{2+}, and Xe^{2+} is given in Table III. Our experimental results show fair agreement with all theoretical estimates of the $^1S_0$ lifetime. Experimentally, one lifetime measurement was reported previously for each of the $^1S_0$ metastable states. Comparison of our results for the lifetimes with the previous measurements shows good agreement for the $^1S_0$ states of Ar^{2+} and Xe^{2+}, whereas our lifetime value for the Kr^{2+} ($^1S_0$) state is about 12% longer than the earlier measurement.

Table IV summarizes the experimental and theoretical values for the natural radiative lifetimes of the $^2P_{1/2}$ and $^2P_{3/2}$ metastable states of the $4s^24p^3$ and $5s^25p^3$ ground-state configurations of Kr^{3+} and Xe^{3+}, respectively. However, because of poor spectral isolation, we were unable to make an unambiguous measurement of the radiative lifetime of the Kr^{3+} ($^2P_{3/2}$) metastable state. Theoretical values for the lifetimes of the $^2P_{1/2}$ and $^2P_{3/2}$ states of Kr^{3+} and Xe^{3+} were obtained from a summation of the $M1$ and $E2$ spontaneous-emission probabilities calculated by Biémont and Hansen [13] and also by Reader [14]. Since the estimated uncertainty associated with the calculated lifetimes is minimally about 10%, our measured lifetimes are in good agreement with the theoretical values.

Finally, for the six metastable states that we observed, Table V gives the collision rate coefficients that result from our investigation of the pressure dependence of the decay rates.

ACKNOWLEDGMENT

We gratefully thank Dr. Joe Reader for permission to list in Table IV his unpublished theoretical values for the radiative lifetimes of the $^2P_{1/2}$ and $^2P_{3/2}$ metastable states of the $4s^24p^3$ and $5s^25p^3$ ground-state configurations of Kr^{3+} and Xe^{3+}, respectively.

* Present address: Harvard-Smithsonian Center for Astrophysics, Cambridge, MA 02138.

[1] C. E. Johnson, J. Appl. Phys. **55**, 3207 (1984).
[2] A. G. Calamai and C. E. Johnson, Phys. Rev. **A 42**, 5425 (1990).
[3] C. E. Moore, *Atomic Energy Levels*, Natl. Bur. Stand. (U.S.), Circ. No. 467 (U.S. GPO, Washington, DC, 1949), Vol. I; (1952), Vol. II; (1958), Vol. III; and references therein.
[4] J. E. Hansen and W. Persson, Phys. Scr. **25**, 487 (1982).
[5] C. Mendoza and C. J. Zeippen, Mon. Not. R. Astron. Soc. **202**, 981 (1983).
[6] S. J. Czyzak and T. K. Krueger, Mon. Not. R. Astron. Soc. **126**, 177 (1963).
[7] E. Biémont and J. E. Hansen, Phys. Scr. **34**, 116 (1986).
[8] R. H. Garstang, J. Res. Natl. Bur. Stand. Sect. **A 68**, 61 (1964).
[9] M. H. Prior, Phys. Rev. A **30**, 3051 (1984).
[10] R. A. Walch and R. D. Knight, Phys. Rev. **A 38**, 2375 (1988).
[11] H. O. DiRocco *et al.*, Phys. Rev. **A 33**, 2114 (1986).
[12] W. Persson and S. G. Pettersson, Phys. Scr. **29**, 308 (1984).
[13] E. Biémont and J. E. Hansen, Phys. Scr. **33**, 117 (1986).
[14] J. Reader (private communication). The calculations were performed using HXR (Hartree exchange with relativity) wave functions with the Hartree-Fock code of R. D. Cowan, *The Theory of Atomic Structure and Spectra* (University of California Press, Berkeley, CA, 1981).
[15] K. H. Kingdon, Phys. Rev. **21**, 408 (1923).
[16] R. H. Hooverman, J. Appl. Phys. **34**, 3505 (1963).
[17] P. R. Bevington, *Data Reduction and Error Analysis for the Physical Sciences* (McGraw-Hill, New York, 1969), Chap. 6.
[18] A. G. Calamai and C. E. Johnson, Phys. Rev. **A 44**, 218 (1991).